Dual periodicities in the rotational modulation of Saturn narrowband emissions

S.-Y. Ye,[1] D. A. Gurnett,[1] J. B. Groene,[1] Z. Wang,[1] and W. S. Kurth[1]

Received 4 June 2010; revised 5 August 2010; accepted 16 September 2010; published 31 December 2010.

[1] Using the Cassini Radio and Plasma Wave Science (RPWS) instrument it has recently been shown that the rotational modulation period of Saturn kilometric radiation (SKR) has two components, one with a period of 10.6 h and the other with a period of 10.8 h. The longer period is primarily observed in the southern hemisphere and the shorter period is primarily observed in the northern hemisphere. In this paper, the modulation period of 5 kHz Saturn narrowband radio emissions is examined, restricting the spacecraft location to either the northern or the southern hemisphere of Saturn. It is found that in both hemispheres, the modulation period of 5 kHz narrowband emissions has two components that are equal to the SKR periods. It is known that Saturn narrowband emissions are first generated in the auroral regions as Z-mode and then mode convert to escaping L-O modes at density gradients. These Z-mode waves are trapped in a region close to the planet and can propagate from one hemisphere to another before they mode convert to L-O modes, thereby leading to dual periods of Saturn narrowband emissions in each hemisphere. The phase shift between the SKR and narrowband emissions is around 90° in the longitude, which means that SKR leads narrowband emissions by 2–3 h.

Citation: Ye, S.-Y., D. A. Gurnett, J. B. Groene, Z. Wang, and W. S. Kurth (2010), Dual periodicities in the rotational modulation of Saturn narrowband emissions, *J. Geophys. Res.*, *115*, A12258, doi:10.1029/2010JA015780.

1. Introduction

[2] For decades, the rotational period of gas giant planets has been determined by analyzing the modulation period of their auroral radio emissions. This approach is based on the belief that the motion of the magnetospheric particles responsible for the generation of these emissions was controlled by the planetary magnetic field, which is linked to the deep interior of the planets. However, the modulation period of Saturn kilometric radiation (SKR), an intense radio emission from Saturn at kilometric wavelengths, which was internationally accepted as the rotational period of Saturn, has been shown to have a small (1%) long-term variation [*Galopeau and Lecacheux*, 2000]. This is also confirmed by the Cassini RPWS observations during the approach to Saturn from 2002 to 2004 [*Gurnett et al.*, 2005]. Recently, using data from Cassini in orbit around Saturn, *Kurth et al.* [2008] discovered a second component in the modulation period of SKR. *Gurnett et al.* [2009a] examined the two components of SKR (10.6 and 10.8h) and found they are associated with the northern and southern hemispheres of Saturn, respectively. Interestingly, *Gurnett et al.* [2009b] showed that Saturn auroral hiss, a broadband whistler mode emission mostly observed at high latitudes in Saturn's magnetosphere at frequencies below about 100 Hz, display a nearly identical north-south asymmetry in its rotational modulation. In this paper, we investigate the existence of a possible north-south asymmetry in the rotational modulation period of Saturn narrowband emissions, which is an L-O mode narrowbanded radio emission most prominent at 5 kHz [*Gurnett et al.*, 1981a; *Louarn et al.*, 2007; *Ye et al.*, 2009; *Wang et al.*, 2010].

[1]Department of Physics and Astronomy, University of Iowa, Iowa City, Iowa, USA.

0148-0227/10/2010JA015780

2. Saturn Narrowband Radio Emissions

[3] Saturn narrowband emissions were first detected during the Voyager 1 flyby of Saturn at around 5 kHz [*Gurnett et al.*, 1981a]. *Louarn et al.* [2007] discussed the similarity between the Kronian narrowband radio emissions with Jovian narrowband emissions (n-KOM) and named the 5 kHz narrowband radio emissions n-SMR. During the Cassini mission, higher frequency (from 10 to 70 kHz) but less intense Saturn narrowband emissions were also detected, which are referred to as 20 kHz narrowband emissions by *Wang et al.* [2010] and *Ye et al.* [2009] and n-SKR by *Lamy et al.* [2008a, 2008b]. Both the 5 and 20 kHz narrowband emissions were found to be propagating in the L-O mode [*Ye et al.*, 2009]. Narrowband emissions are detected at all latitudes and local times covered by Cassini, except probably when the dense part of the plasma torus lies between the source and the spacecraft so the L-O mode waves gets reflected [*Wang et al.*, 2010]. The 5kHz narrowband emissions is modulated near the rotational period of Saturn and the rotational modulation resembles that of SKR, which has a clock-like source [*Wang et al.*, 2010].

[4] Many different mechanisms have been proposed for the generation of Saturn narrowband emissions. *Gurnett et al.*

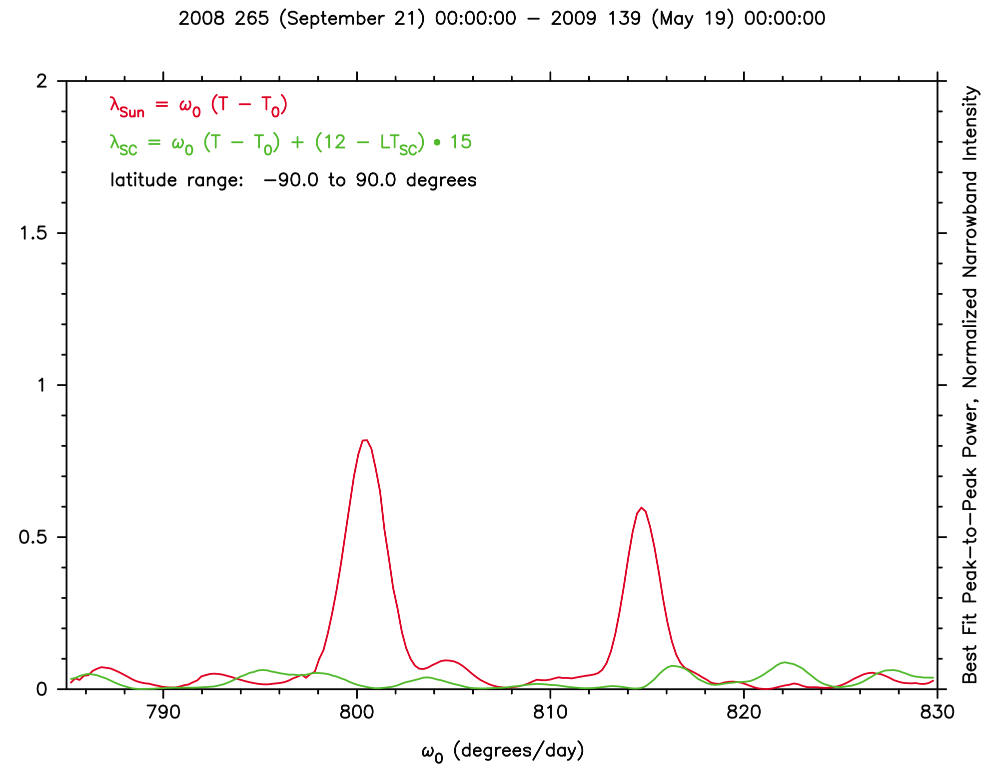

Figure 1. Spectrum analysis of the modulation period of 5 kHz Saturn narrowband emissions under the assumption of a clock-like source (red) or rotating beam source (green).

[1981a] proposed that Saturn narrowband emissions are mode converted from electrostatic upper hybrid waves excited near the boundary of the plasma torus via either a linear [*Jones*, 1976] or a nonlinear mechanism [*Melrose*, 1981]. *Ye et al.* [2009] showed that the generation of the 20 kHz narrowband emissions is consistent with the mode conversion theory. More recently, *Ye et al.* [2010] put forth the idea that the 5 kHz L-O mode narrowband emission is mode converted from Z-mode waves detected mainly in the low-density region between Saturn and the plasma torus. The wave growth analysis, based on the electron distribution function measured near a possible source region, indicated that electromagnetic Z-mode waves could be excited by cyclotron maser instability when the local upper hybrid frequency is close to the harmonics of local electron cyclotron frequency, that is, nf_{ce} (n = 2, 3,…) [*Menietti et al.*, 2009; *Menietti et al.*, 2010]. Additional support for this mechanism is given by the fact that no intense electrostatic upper hybrid waves have been observed around the predicted source locations given by the *Ye et al.* [2009] model based on the mode conversion theory. So it is likely that the Saturn narrowband emissions are first generated as electromagnetic Z-mode waves and then mode convert to L-O mode at a density gradient or density irregularities.

3. Modulation of Saturn Narrowband Emissions

[5] It has been shown that the intensity of SKR has a clock-like (or flashing light) modulation, which means SKR intensity reaches its maximum whenever a certain SKR longitude rotates to the subsolar point, independent of the location of Cassini with respect to Saturn [*Warwick et al.*, 1981; *Gurnett et al.*, 1981b]. In contrast, the modulation of the intensity of Saturn auroral hiss has been found to resemble a rotating beacon (or search light) [*Gurnett et al.*, 2009b]. This indicates that auroral hiss is a beamed signal that is constantly on at a certain longitude. Therefore it is only observable when the spacecraft flies through the beam. *Wang et al.* [2010] showed that the 5 kHz Saturn narrowband emission has a clock-like source. This means that narrowband emissions are triggered periodically, possibly when a longitudinal anomaly rotates to certain local time of Saturn's magneosphere. Additionally, narrowband emissions are not narrowly beamed so that they can be observed from a wide range of longitudes and local times.

[6] To determine the modulation period of Saturn narrowband emissions, we employ the same method *Gurnett et al.* [2009a] developed to analyze the rotational modulation of SKR. The 5 kHz narrowband emissions are mainly observed by the High Frequency Receiver (HFR) of Cassini Radio and Plasma Wave Science (RPWS) instrument [*Gurnett et al.*, 2004; *Gurnett et al.*, 2005]. The first step is to integrate the HFR received power spectral density between 3 and 8 kHz, the frequency range over which 5 kHz narrowband emissions are normally observed. To calculate the power flux for each frequency channel, we divide the measured intensity (volts squared per hertz) with the square of effective antenna length (listed in *Vogl et al.* [2001]) to get the electric field power spectrum density (volts squared per square meters-hertz). Then we multiply the sum of the electric field power spectral densities on both the dipole (X [or u for the direction finding mode]) and the monopole antenna (w) with the frequency bandwidth. The result is then divided by 377 Ω (the impedance of free space) to get the power flux in watts per

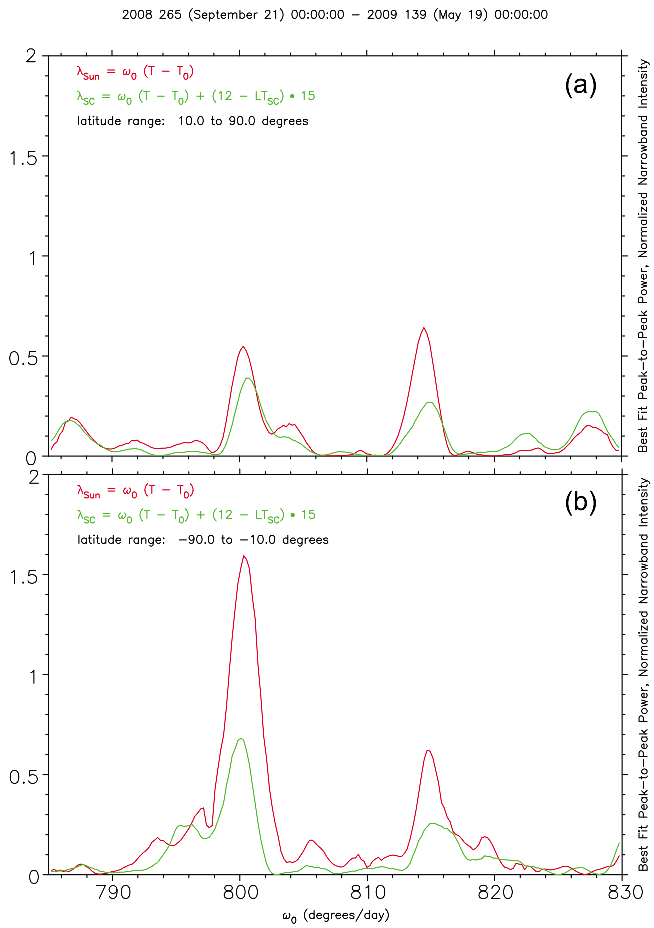

Figure 2. Spectrum analysis of the modulation period of 5 kHz Saturn narrowband emissions observed in the (a) northern hemisphere and (b) southern hemisphere.

square meters [*Zarka et al.*, 2004]. The integrated narrowband emission intensities are normalized over one rotation period to account for the periodical variations in the intensity due to the $1/R^2$ dependence on the radial distance, R, from the planet. The next step is to compute the rotational modulation spectrum. To limit the spectrum analysis to a certain period, the normalized intensities are multiplied by a Hanning weighting function [*Priestly*, 1981], where the duration of the window has been chosen to be 240 days. The 240 day window also guarantees an accuracy better than 1% for the determined period of modulation. The normalized and weighted intensities of narrowband emissions are then sorted and averaged in 1° longitudinal bins, assuming different rotation rates, ω. For each ω the resulting averages are fit to a sinusoidal function of longitude, $A\sin[2\pi\ (\lambda - \phi)/360°]$, thereby providing the amplitude, A, and phase, ϕ, of the modulation.

[7] In Figure 1, we plot the normalized modulation power, P [$P = (2A)^2$], versus the assumed rotation rate. Each point on the spectrum curve corresponds to a sine wave fit described above. To confirm the clock-like modulation of narrrowband emissions, two longitude systems are used during the analysis. For a clock-like source (red) the intensities are sorted into bins of longitude of the Sun, $\lambda_{\rm Sun} = \omega T$, where T is the Universal Time (UT) at the spacecraft. For a rotating beam source (green), the intensities are sorted into the bins of longitude of the spacecraft, $\lambda_{\rm SC} = \omega T + (12 - {\rm LT_{SC}}) \times 15°$, where $\rm LT_{SC}$ is the local time of the spacecraft. Figure 1 shows that the modulation power P of narrowband emissions has two peaks near the periods around 800 and 815 degrees per day based on the assumption of a clock-like source (red), whereas no obvious peaks are found for the rotating beacon source assumption (green). This clearly confirms the result of *Wang et al.* [2010] that Saturn narrowband emissions has a clock-like source.

[8] To investigate the existence of a possible north-south asymmetry in the rotational modulation period of Saturn narrowband emissions, we divide our data set into two sets, one for narrowband emissions observed at latitudes greater than 10°, and the other for latitudes less than −10°, similar to the way *Gurnett et al.* [2009a] differentiated the radiations from northern and southern sources of SKR. Unlike the case of SKR, where a north-south asymmetry was clearly revealed, the narrowband emissions display both modulation periods (800 and 815 degrees per day) in each hemisphere, which is shown in Figure 2. This result remains the same for other periods analyzed. Similar results are obtained if we change the equatorial exclusion threshold from ±10° to ±20° or ±30°. It is noted in Figure 2a that the peaks of modulation power under the assumption of rotating beam source (green) is somewhat comparable to the peaks of modulation power under the clock-like source assumption. This is probably due to the limited local time coverage, which is crucial to distinguishing the two types of source modulation, when we restrict the latitude of the observations.

4. Indistinguishable Source Hemispheres

[9] The fact that 5 kHz narrowband emissions do not show a north-south asymmetry in their rotational modulation can be explained by the way narrowband emissions are generated. *Ye et al.* [2010] showed that Saturn narrowband emissions are mode converted from Z-mode waves that are trapped between propagation cutoffs at upper hybrid frequency f_{UH} and left-hand cutoff frequency $f_{L=0}$. These electromagnetic Z-mode waves are refracted and guided by the cutoff surfaces as they propagate such that they can cross the equator either inside or outside the Enceladus plasma torus where the plasma density is low. At a density gradient or density irregularities, these Z-mode waves can mode convert to L-O mode and escape the trapping region. As a result, the modulated signals from both hemispheres can be observed in one hemisphere. In contrast, the propagation of SKR and auroral hiss are relatively restricted to the same hemisphere they are generated in. According to cyclotron maser instability theory, SKR is mainly generated as R-X mode near the local electron cyclotron frequency f_{ce} in the source [*Wu and Lee*, 1979]. The theory also predicts that SKR propagates along a cone surface centered along the local magnetic field line. Figure 2 of *Lamy et al.* [2008b] shows that the propagation of SKR remains in the same hemisphere they are generated in. SKR generated at the lowest frequencies (e.g., 10 kHz), although beamed toward high latitudes of the other hemisphere, cannot cross the equator due to the refraction by the plasma torus. In the equatorial region where SKR from both hemispheres can be observed, we need information on the wave polarization or the direction of arrival to distinguish

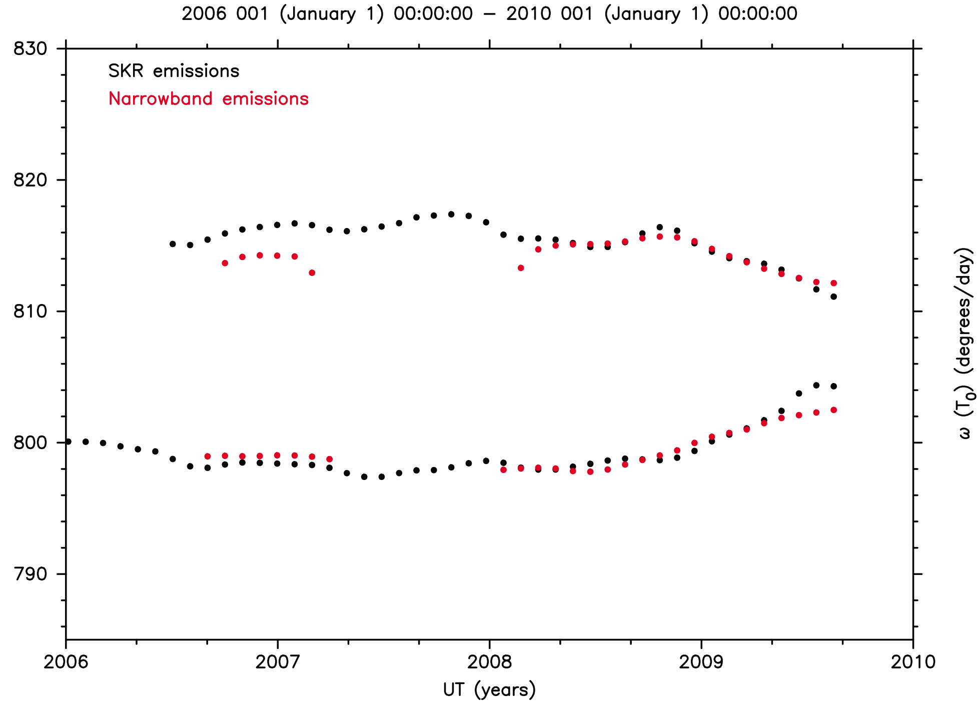

Figure 3. SKR versus narrowband modulation periods from 2006 to 2010. The red dots represent the periods of Saturn narrowband emissions. The black dots represent the periods of SKR given by *Gurnett et al.* [2009a].

between the northern and southern source of SKR. However, if we restrict the observations to high northern/southern latitudes, as in *Gurnett et al.* [2009a], SKR emitted by the northern/southern sources can be selected. Auroral hiss is believed to be generated by a coherent beam-plasma interaction [*Maggs*, 1976] via Landau resonance, $\omega/k_{\|} = v_{\|}$. The low energy of the electrons involved in the generation of auroral hiss requires that the wave normal of the whistler mode waves remain close to the resonance cone [*Gurnett and Frank*, 1972]. The resulting propagation path is a filled cone centered along the magnetic field line with higher frequency auroral hiss propagating at a larger angle with respect to the local magnetic field. The funnel shape of auroral hiss on a spectrogram also arises from this propagation effect. Because auroral hiss is a whistler mode wave that can only propagate below the plasma frequency, it cannot escape the source region like SKR, which is generated in the R-X or L-O mode and can propagate as far as their respective low-frequency cutoffs are locally reached. Because it is easy to distinguish Saturn auroral hiss from different hemispheres, by restricting the latitude of observation, we can reveal the north-south asymmetry with the modulation analysis. The same is true for SKR, but for Saturn narrowband emissions, this is impossible.

5. Comparison to Saturn Kilometric Radiation

[10] *Gurnett et al.* [2009b] has shown that the modulation period of auroral hiss in a given hemisphere is consistent with the modulation period of SKR in that hemisphere. Figure 3 shows a comparison of the rotational modulation rates of Saturn narrowband emission and SKR. The red dots in Figure 3 represent the modulation rates of Saturn narrowband emissions which are obtained from the modulation spectrum analysis described in section 3. For the time range when few narrowband emissions are observed, for example, from 2004 to 2006 and late 2007, the modulation rates are not determined, hence no red dots. The black dots represent the modulation rates of SKR given by *Gurnett et al.* [2009a]. The SKR periods are determined throughout the 6 years of study because SKR is observed continuously. Note that the second period of SKR, which is associated with the northern hemisphere of Saturn, only appears after the middle of 2006. This is because Cassini spent most of the time on the equatorial or slightly southern latitudes from 2004 to 2006, so the periodic signal of SKR from the northern hemisphere was not observed. During the time when Saturn narrowband emissions and SKR were both continuously observed, the modulation rates of Saturn narrowband emissions are nearly identical to those of SKR. There are exceptions though, when the red dots are more than 2° per day off the black dots, for example, the northern periods from late 2006 to early 2007 and early 2008. These gaps between the rotation rates of SKR and narrowband emissions in the northern hemisphere are still poorly understood. The possible cause for them will be discussed later.

[11] *Louarn et al.* [2007] presented the integrated flux of 5 kHz narrowband emissions as a function of Saturn longitude. Their Figure 3 showed a systematical drift in longitude from one narrowband emission to the next in the sense of super corotation. The shift in phase of narrowband emissions indicated a 5% super corotation (i.e., ~40° per day). This is not consistent with the result of this paper, where the narrowband modulation rates are no more than a few degrees per day off the SKR rates.

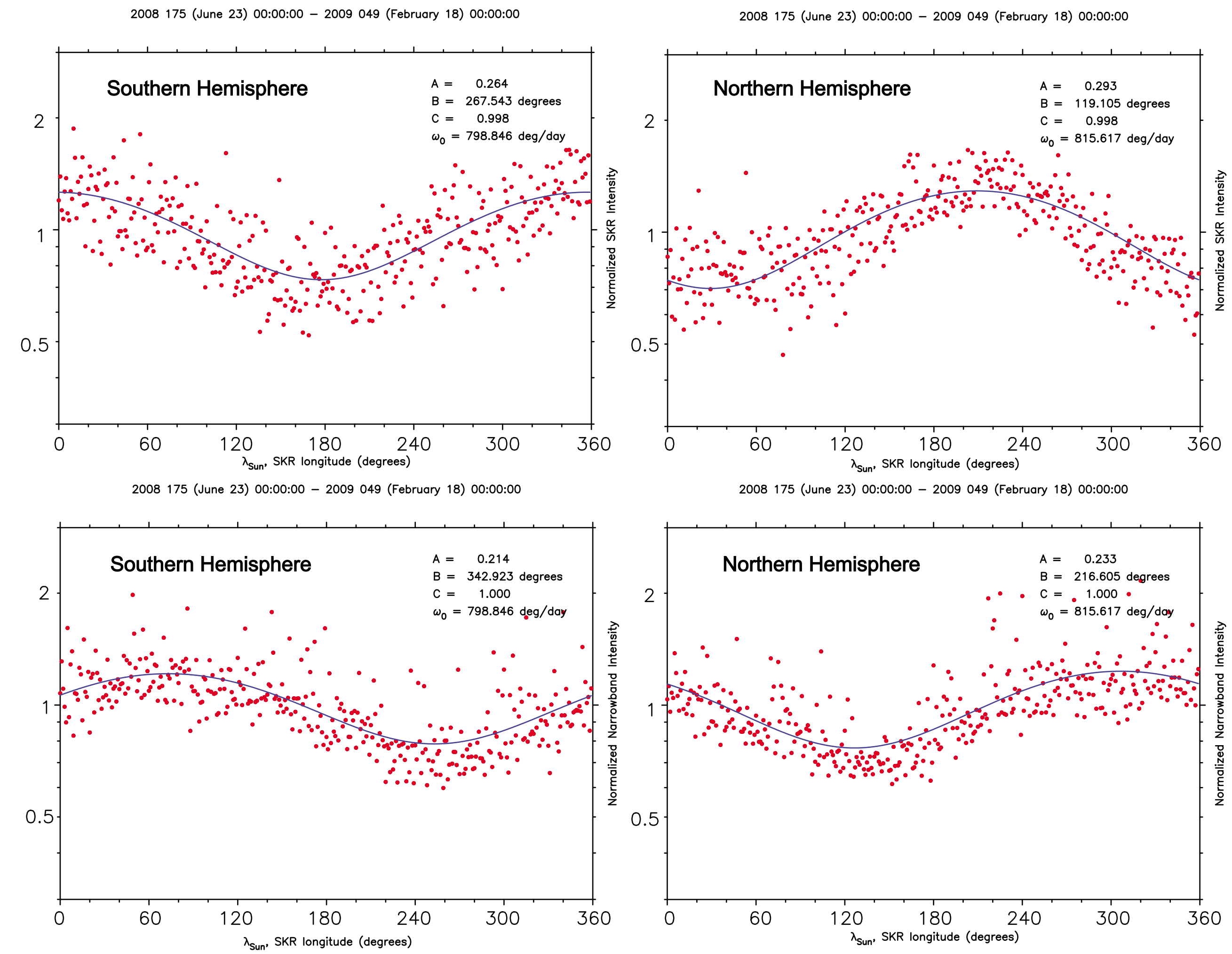

Figure 4. The phase difference between (top) SKR and (bottom) narrowband emissions in both (left) southern and (right) northern hemispheres, measured by directly comparing the sine function fits of the normalized SKR and narrowband emission intensities (the red dots).

[12] *Gurnett et al.* [2009b] analyzed the phase difference between SKR and Saturn auroral hiss and concluded that the auroral hiss source is rotating through the local afternoon side of the magnetosphere when SKR reaches maximum intensity in the late morning sector of the magnetosphere. Since Saturn narrowband emissions are also modulated at nearly the same rates as SKR, we can analyze the phase shift between SKR and narrowband emissions in the northern and southern hemispheres separately. This is done by directly comparing the sine function fits of the intensities of SKR and narrowband emissions based on the previously determined northern and southern hemisphere periods. Figure 4 shows that between day of year (DOY) 175 of 2008 and DOY 049 of 2009, the phase difference between SKR and narrowband emissions is around 90° in both northern and southern hemispheres.

[13] Figure 5 shows the evolution of the phase shift between Saturn narrowband emissions and SKR, for the northern and southern hemispheres separately. Each dot in this figure represents a measurement over 240 days of the phase shift between 5 kHz narrowband emissions and SKR. The vertical coordinate of each dot represents the phase shift between SKR and narrowband emissions, obtained by subtracting the phase angle of SKR from that of narrowband emissions. For example, a positive 90° phase shift indicates that the narrowband emissions reach maximum intensities one quarter of a rotational period after the maximum of SKR. The phase shift stays relatively constant for the time interval when the modulation rates of narrowband emissions and SKR are identical. For example, from 2008 to early 2009, for the northern hemisphere, the phase shift remained around 80°–120°. When the difference between the modulation rates of narrowband emissions and SKR are nonnegligible, the phase shift between them changes very fast, because the rate of change is equal to the difference in the modulation rates of SKR and narrowband emissions. This is clearly seen in Figure 5, where the time intervals with steep slopes in data points correspond to the times when the measured SKR and narrowband emission periods are not identical (see Figure 3). In the following discussion, we focus on the part of data where the phase shift is relatively stable.

[14] Figure 6 shows the occurrence rate of narrowband emissions during each 240 day window. The occurrence rate is estimated by dividing the number of data points where

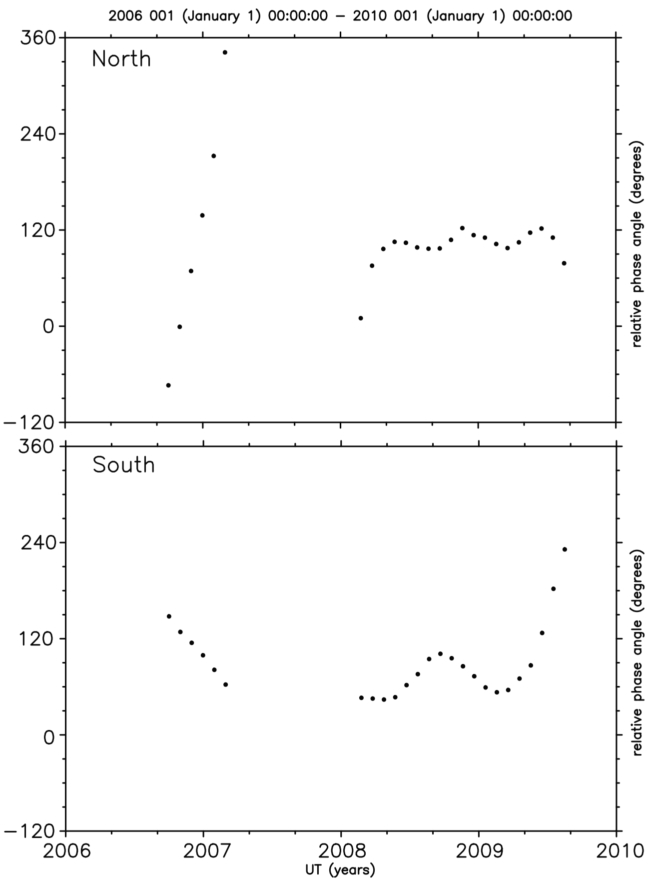

Figure 5. The phase difference between SKR and narrowband emissions in both (top) northern and (bottom) southern hemispheres versus time.

narrowband emissions are observed within 10 h intervals by the total possible number of data points within the 240 day window. For the interval (2008–2009) with higher occurrence rate (50+%) of narrowband emissions, the rotational modulation rates of narrowband emissions follow the SKR rates closely. Note that the points in Figure 6 with occurrence rates lower than 40% correspond to the intervals in Figure 3 where no modulation rates of narrowband emissions are determined. From 2006 to 2007, the occurrence rate of narrowband emissions is just over the threshold of 40% for the determination of rotation rates, which suggests a greater uncertainty in the determined rotation rates. The discontinuity of the data is also similar to the effect of rectangular window in the spectrum analysis, which means the leakage of power from the southern peak (assume the northern hemisphere signal is relatively weak compared to the southern hemisphere signal) can affect the location of the northern peak. So the gap between the modulation rates of SKR and narrowband emissions could be caused by the lower occurrence rate of narrowband emissions during the analysis period.

[15] It is known that both SKR and Saturn narrowband emissions are modulated like a clock. SKR reaches its maximum intensity when the rotating plasma feature goes through the morning sector of Saturn's magnetosphere [*Gurnett et al.* 2007; *Cecconi et al.*, 2009; *Lamy et al.*, 2009], perhaps due to the enhanced field aligned current induced by the pressure gradient from the asymmetric ring current [*Mitchell et al.*, 2009]. If Saturn narrowband emissions were associated with the same rotating plasma feature that is responsible for the generation of SKR [*Wang et al.*, 2010], they should be excited when the plasma feature rotates to the dusk side of the planet, according to the 90° phase shift between SKR and narrowband emissions.

6. Discussion

[16] Cassini observations since Saturn orbit insertion have revealed planetary spin periodic perturbations in magnetic field [*Southwood and Kivelson*, 2007; *Andrews et al.*, 2008], radio emissions [*Galopeau and Lecacheux*, 2000; *Gurnett et al.*, 2005; *Kurth et al.*, 2007], particle measurements [*Krupp et al.*, 2005; *Carbary et al.*, 2007], auroral oval location [*Nichols et al.*, 2008], and magnetopause boundary [*Clarke et al.*, 2006]. These rotational modulations are hard to explain due to the lack of magnetic dipole tilt angle with respect to Saturn's rotational axis. *Espinosa et al.* [2003] proposed a cam-shaft model in which a corotating longitudinal asymmetry can induce a compressional wave that propagates radially outward, thus imposing the planet's rotational period over the entire magnetosphere of Saturn.

[17] *Gurnett et al.* [2007] reported the occurrence of a rotational modulation of the cold plasma density and magnetic field near the orbit of Enceladus that is phase locked to the time-variable SKR modulation. They proposed a two-cell corotating convection pattern with stronger centrifugally driven plasma outflow on its dense side which acts as the cam. This plasma outflow can then break the axisymmetry of the external magnetic field at Saturn and drive other planetary period modulated magnetospheric effects such as SKR [*Goldreich and Farmer*, 2007]. *Khurana et al.* [2009] clarified that the "cam" source is actually the ring current anomaly often revealed by the enhancement of energetic neutral atom (ENA) emissions. *Mitchell et al.* [2009] associated the ENA enhancement events with bursts of SKR and dawn-side transient auroral brightenings and argued that the rotating azimuthal asymmetry of the ring current pressure induces a rotating field-aligned current system that drives the auroral processes.

[18] *Provan et al.* [2009] examined the polarization characteristics of magnetic field oscillations in the northern and southern polar regions and found that the overall pattern of field perturbations are consistent with a rotating partial ring current and its field-aligned closure currents. These currents are stronger in the southern hemisphere due to the better ionospheric conductivity in the southern ionosphere during the southern summer conditions. As a result, there is a difference of momentum transfer from the magnetosphere to the atmosphere between the northern and southern hemispheres, which according to *Gurnett et al.* [2009a], is the cause of the north-south asymmetry in the rotational modulation period of SKR. Interestingly, *Carbary et al.* [2009] found that energetic electron fluxes also display dual periodicities similar to SKR but with the longer 10.8 h period observed in both hemispheres and the shorter 10.6 h period observed only in the northern hemisphere. The dual periodicity in narrowband emissions discussed in this paper should also be caused by the same north-south asymmetry that causes the dual periodicity in SKR and energetic electrons. However, since the Z-mode waves can cross the equator before they mode

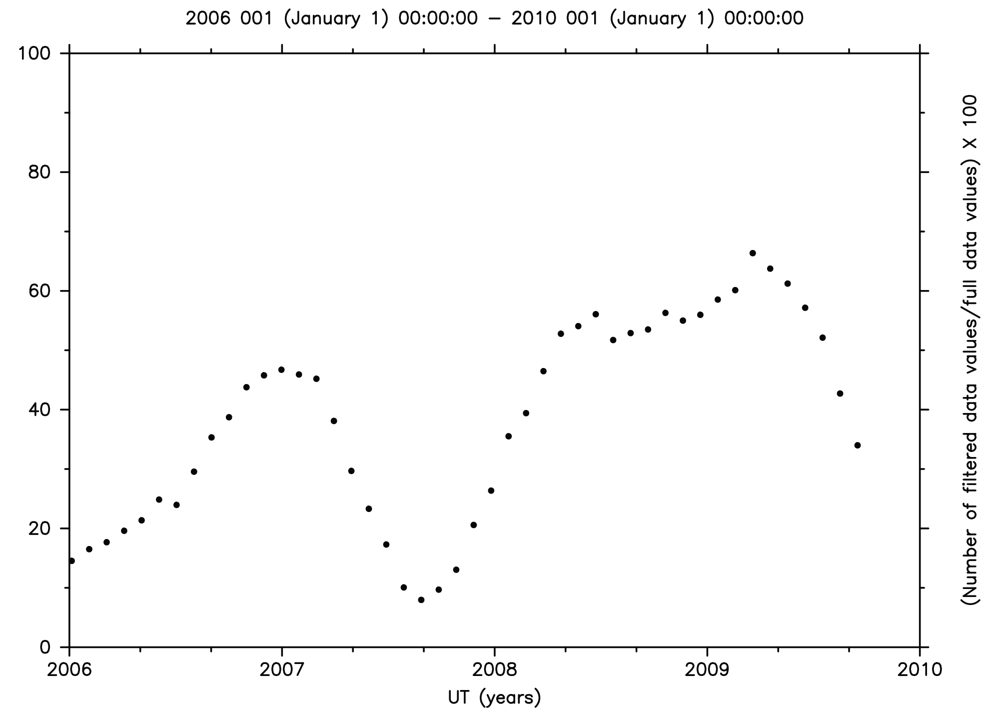

Figure 6. Occurrence rate of narrowband emissions during each 240 day window.

convert to L-O mode narrowband emissions and escape, it is impossible to select the source hemispheres by restricting the latitude of observations.

[19] SKR is generated by the upward field-aligned current which connects the equatorial enhanced partial ring current to the ionosphere. In the model discussed by *Provan et al.* [2009], the SKR power reaches maximum when the upward field-aligned current rotates to the early morning sector, with the enhanced ring current on the day side. From Figure 11a of *Provan et al.* [2009], it can be seen that upward field-aligned currents are in approximately lagging quadrature to the ring current maximum. As shown in the previous section, the narrowband emissions lag SKR by about 90° in terms of the longitude of the Sun. If the asymmetric ring current is the cam that perturbs the rest of the magnetosphere and triggers periodical radio emissions, then the maximum of the partial ring current would have rotated to the dusk sector when the 5 kHz narrowband emissions are triggered. It should be noted that the cold plasma density modulation in the torus discovered by *Gurnett et al.* [2007] is in phase with the "core" azimuthal magnetic field perturbation, which is associated with the downward field-aligned current region. So the maximum of the cold plasma torus is in leading quadrature with the maximum phase of the ring current.

7. Conclusions

[20] We analyzed the periodic behavior of Saturn narrowband emissions and its relation to the rotationally modulated SKR. We confirmed that the rotational modulation of 5 kHz Saturn narrowband emissions is a clock-like modulation. Similar to SKR, the 5 kHz Saturn narrowband emissions also display two distinct modulation periods, which are identical to the the north and south periods of SKR. However, both of these two narrowband modulation periods are observable in each hemisphere of Saturn, which is contrary to the north-south asymmetry in the case of SKR. One interpretation of this contradiction is that the 5 kHz narrowband emissions are first generated as Z-mode waves, which are trapped in an electron density cavity between Saturn and the plasma torus. These Z-mode waves can propagate from hemisphere to hemisphere within the low density cavity before the mode conversion to L-O mode, leading to the dual periodicity of narrowband emissions in each hemisphere. For the time interval when the modulation rates of narrowband emissions and SKR are identical, the phase shift between the SKR and narrowband emissions remains relatively constant, which is about 90° in the longitude. This means that SKR leads the narrowband emissions by about 2–3 h. This puts the triggering location of narrowband emissions at late afternoon or the dusk side of the planet, if the enhanced partial ring current is responsible for the generation of narrowband emissions.

[21] **Acknowledgments.** The research reported in this paper was supported by NASA and the Cassini project through contract 1279973 from the Jet Propulsion Laboratory.

[22] Philippa Browning thanks the reviewers for their assistance in evaluating this paper.

References

Andrews, D. J., E. J. Bunce, S. W. H. Cowley, M. K. Dougherty, G. Provan, and D. J. Southwood (2008), Planetary period oscillations in Saturn's magnetosphere: Phase relation of equatorial magnetic field oscillations and Saturn kilometric radiation modulation, *J. Geophys. Res.*, *113*, A09205, doi:10.1029/2007JA012937.

Carbary, J. F., D. G. Mitchell, S. M. Krimigis, D. C. Hamilton, and N. Krupp (2007), Spin-period effects in magnetospheres with no axial tilt, *Geophys. Res. Lett.*, *34*, L18107, doi:10.1029/2007GL030483.

Carbary, J. F., D. G. Mitchell, S. M. Krimigis, and N. Krupp (2009), Dual periodicities in energetic electrons at Saturn, *Geophys. Res. Lett.*, *36*, L20103, doi:10.1029/2009GL040517.

Cecconi, B., L. Lamy, P. Zarka, R. Prangé, W. S. Kurth, and P. Louarn (2009), Goniopolarimetric study of the revolution 29 perikrone using the Cassini Radio and Plasma Wave Science instrument high-frequency radio receiver, *J. Geophys. Res.*, *114*, A03215, doi:10.1029/2008JA013830.

Clarke, K. E., et al. (2006), Cassini observations of planetary-period oscillations of Saturn's magnetopause, *Geophys. Res. Lett.*, *33*, L23104, doi:10.1029/2006GL027821.

Espinosa, S. A., D. J. Southwood, and M. K. Dougherty (2003), How can Saturn impose its rotation period in a noncorotating magnetosphere?, *J. Geophys. Res.*, *108*(A2), 1086, doi:10.1029/2001JA005084.

Galopeau, P., and A. Lecacheux (2000), Variations of Saturn's radio rotation period measured at kilometer wavelengths, *J. Geophys. Res.*, *105*(A6), doi:10.1029/1999JA005089.

Goldreich, P., and A. J. Farmer (2007), Spontaneous axisymmetry breaking of the external magnetic field at Saturn, *J. Geophys. Res.*, *112*, A05225, doi:10.1029/2006JA012163.

Gurnett, D. A., and L. A. Frank (1972), VLF hiss and related plasma observations in the polar magnetosphere, *J. Geophys. Res.*, *77*(1), 172–190.

Gurnett, D. A., W. S. Kurth, and F. L. Scarf (1981a), Narrowband electromagnetic emissions from Saturn's magnetosphere, *Nature*, *292*, 733.

Gurnett, D. A., W. S. Kurth, and F. L. Scarf (1981b), Plasma waves near Saturn: Initial results from Voyager 1, *Science*, *212*, 235–239.

Gurnett, D. A., et al. (2004), The Cassini radio and plasma wave investigation, *Space Sci. Rev.*, *114*, 395.

Gurnett, D. A., et al. (2005), Radio and plasma wave observations at Saturn from Cassini's approach and first orbit, *Science*, *307*, 1255, doi:10.1126/science.1105356.

Gurnett, D. A., A. M. Persoon, W. S. Kurth, J. B. Groene, T. F. Averkamp, M. K. Dougherty, and D. J. Southwood (2007), The variable rotation period of the inner region of Saturn's plasma disk, *Science*, *316*, 442.

Gurnett, D. A., A. Lecacheux, W. S. Kurth, A. M. Persoon, J. B. Groene, L. Lamy, P. Zarka, and J. F. Carbary (2009a), Discovery of a north-south asymmetry in Saturn's radio rotation period, *Geophys. Res. Lett.*, *36*, L16102, doi:10.1029/2009GL039621.

Gurnett, D. A., A. M. Persoon, J. B. Groene, A. J. Kopf, G. B. Hospodarsky, and W. S. Kurth (2009b) A north-south difference in the rotation rate of auroral hiss at Saturn: Comparison to Saturn's kilometric radio emission, *Geophys. Res. Lett.*, *36*, L21108, doi:10.1029/2009GL040774.

Jones, D. (1976), Source of terrestrial nonthermal radiation, *Nature*, *260*, 686.

Khurana, K. K., D. G. Mitchell, C. S. Arridge, M. K. Dougherty, C. T. Russell, C. Paranicas, N. Krupp, and A. J. Coates (2009), Sources of rotational signals in Saturn's magnetosphere, *J. Geophys. Res.*, *114*, A02211, doi:10.1029/2008JA013312.

Krupp, N., et al. (2005), The Saturnian plasma sheet as revealed by energetic particle measurements, *Geophys. Res. Lett.*, *32*, L20S03, doi:10.1029/2005GL022829.

Kurth, W. S., A. Lecacheux, T. F. Averkamp, J. B. Groene, and D. A. Gurnett (2007), A Saturnian longitude system based on a variable kilometric radiation period, *Geophys. Res. Lett.*, *34*, L02201, doi:10.1029/2006GL028336.

Kurth, W. S., T. F. Averkamp, D. A. Gurnett, J. B. Groene, and A. Lecacheux (2008), An update to a Saturnian longitude system based on kilometric radio emissions, *J. Geophys. Res.*, *113*, A05222, doi:10.1029/2007JA012861.

Lamy, L., P. Zarka, B. Cecconi, R. Prangé, W. S. Kurth, and D. A. Gurnett (2008a), Saturn kilometric radiation: Average and statistical properties, *J. Geophys. Res.*, *113*, A07201, doi:10.1029/2007JA012900.

Lamy, L., P. Zarka, B. Cecconi, S. Hess, and R. Prangé (2008b), Modeling of Saturn kilometric radiation arcs and equatorial shadow zone, *J. Geophys. Res.*, *113*, A10213, doi:10.1029/2008JA013464.

Lamy, L., B. Cecconi, R. Prangé, P. Zarka, J. D. Nichols, and J. T. Clarke (2009), An auroral oval at the footprint of Saturn's kilometric radio sources, colocated with the UV aurorae, *J. Geophys. Res.*, *114*, A10212, doi:10.1029/2009JA014401.

Louarn, P., et al. (2007), Observation of similar radio signatures at Saturn and Jupiter: Implications for the magnetospheric dynamics, *Geophys. Res. Lett.*, *34*, L20113, doi:10.1029/2007GL030368.

Maggs, J. E. (1976), Coherent generation of VLF hiss, *J. Geophys. Res.*, *81*, 1707–1724.

Melrose, D. B. (1981), A theory for the nonthermal radio continua in the terrestrial and Jovian magnetospheres, *J. Geophys. Res.*, *86*(A1), 30–34.

Menietti, J. D., S.-Y. Ye, P. H. Yoon, O. Santolik, A. M. Rymer, D. A. Gurnett, and A. J. Coates (2009), Analysis of narrowband emission observed in the Saturn magnetosphere, *J. Geophys. Res.*, *114*, A06206, doi:10.1029/2008JA013982.

Menietti, J. D., P. H. Yoon, S.-Y. Ye, B. Cecconi, and A. M. Rymer (2010), Source mechanism of Saturn narrowband emission, *Ann. Geophys.*, *28*, 1013–1021.

Mitchell, D. G., et al. (2009), Recurrent energization of plasma in the midnight-to-dawn quadrant of Saturn's magnetosphere, and its relationship to auroral UV and radio emissions, *Planet. Space Sci.*, *57*, 1732–1742.

Nichols, J. D., J. T. Clarke, S. W. H. Cowley, J. Duval, A. J. Farmer, J.-C. Gérard, D. Grodent, and S. Wannawichian (2008), Oscillation of Saturn's southern auroral oval, *J. Geophys. Res.*, *113*, A11205, doi:10.1029/2008JA013444.

Priestly, M. B. (1981), *Spectral Analysis and Time Series*, 443 pp., Academic Press, London.

Provan, G., D. J. Andrews, C. S. Arridge, A. J. Coates, S. W. H. Cowley, S. E. Milan, M. K. Dougherty, and D. M. Wright (2009), Polarization and phase of planetary-period magnetic field oscillations on high-latitude field lines in Saturn's magnetosphere, *J. Geophys. Res.*, *114*, A02225, doi:10.1029/2008JA013782.

Southwood, D. J., and M. G. Kivelson (2007), Saturnian magnetospheric dynamics: Elucidation of a camshaft model, *J. Geophys. Res.*, *112*, A12222, doi:10.1029/2007JA012254.

Vogl, D. F., B. Cecconi, W. Macher, et al. (2001), In-flight calibration of the Cassini-Radio and Plasma Wave Science (RPWS) antenna system for direction-finding and polarization measurements, *J. Geophys. Res.*, *109*, A09S17, doi:10.1029/2003JA010261.

Wang, Z., D. A. Gurnett, G. Fischer, S.-Y. Ye, W. S. Kurth, D. G. Mitchell, C. T. Russell, and J. S. Leisner (2010), Narrowband radio emissions and their relationship to rotating plasma clouds and magnetic disturbances at Saturn, *J. Geophys. Res.*, *115*, A06213, doi:10.1029/2009JA014847

Warwick, J. W., et al. (1981), Planetary radio astronomy observations from Voyager 1 near Saturn, *Science*, *212*, 239–243.

Wu, C. S., and L. C. Lee (1979), A theory of the terrestrial kilometric radiation, *Astrophys. J., Part 1*, *230*, 621–626, doi:10.1086/157120.

Ye, S.-Y., D. A. Gurnett, G. Fischer, B. Cecconi, J. D. Menietti, W. S. Kurth, Z. Wang, G. B. Hospodarsky, P. Zarka, and A. Lecacheux (2009), Source locations of narrowband radio emissions detected at Saturn, *J. Geophys. Res.*, *114*, A06219, doi:10.1029/2008JA013855.

Ye, S.-Y., J. D. Menietti, G. Fischer, Z. Wang, B. Cecconi, D. A. Gurnett, and W. S. Kurth (2010), Z mode waves as the source of Saturn narrowband radio emissions, *J. Geophys. Res.*, *115*, A08228, doi:10.1029/2009JA015167.

Zarka, P., B. Cecconi, and W. S. Kurth (2004), Jupiter's low-frequency radio spectrum from Cassini/Radio and Plasma Wave Science (RPWS) absolute flux density measurements, *J. Geophys. Res.*, *109*, A09S15, doi:10.1029/2003JA010260.

J. B. Groene, D. A. Gurnett, W. S. Kurth, Z. Wang, and S.-Y. Ye, Department of Physics and Astronomy, University of Iowa, Iowa City, IA 52242, USA. (Shengyi-Ye@uiowa.edu)